EAST EUROPEAN JOURNAL OF PHYSICS. 4. 542-549 (2025)
DOI:10.26565/2312-4334-2025-4-56 ISSN 2312-4334

SECOND HARMONIC GENERATION OF HIGH-POWER ELLIPTICAL BEAM IN THERMAL QUANTUM PLASMA

Keshav Walia[1]*, Kulkaran Singh[1], Anuj Vijay[2], Deepak Tripathi[3]
[1]*Department of Physics, DAV University Jalandhar, India*
[2]*Department of Physics, GLA University Mathura (U.P.), India-281406*
[3]*Physics Department, USAR, Guru Gobind Singh Indraprastha University, East Delhi Campus, Delhi, India-110032*
**Corresponding Author e-mail: keshavwalia86@gmail.com*
Received September 2, 2025; revised November 9, 2025; accepted November 17, 2025

The current study investigates second harmonic generation of elliptical beam in thermal quantum plasma (TQP) by taking relativistic-ponderomotive (RP) forces together. There is change in mass of electrons due to RP force thereby producing change in background density profile in a direction transverse to main beam. The main beam gets self-focused. The established density gradients excites electron plasma wave (EPW) at pump wave frequency. The excited EPW further interacts with pump wave to produce second harmonic generation (SHG). The widely accepted WKB and paraxial approximations are employed for deriving the 2nd order ODEs for semi major and semi-minor axes of elliptical beam with normalized propagation distance and efficiency of second harmonics. Furthermore, the influence of varying suitable laser-plasma parameters on beam waist dynamics and efficiency of 2nd harmonics are also explored.
Keywords: *Elliptical Cross-section; Quantum Plasma; RP force; Electron Plasma Wave; Paraxial Theory; WKB approximation*
PACS: 52.38.Hb, 52.35.Mw, 52.38.Dx

1. INTRODUCTION

The laser-plasma interaction is vibrant research field as a result of its direct relevance to many applications including X-ray lasers, laser induced, and acceleration of plasma species [1-8]. Recent advancement in laser technology has made possible the production of lasers with intensities exceeding $10^{18}\ W/cm^2$. At such intensity, intense lasers interaction with plasmas has led to interesting nonlinear physics. Because, in this region the behavior of plasma electrons is highly nonlinear. The laser-plasma interaction has led to production of nonlinear phenomena including harmonics production, scattering instabilities, self-focusing and filamentation [9-17]. The complete knowledge of laser-plasma interaction physics requires investigation of these instabilities. These instabilities cause great reduction in efficiency of laser-plasma coupling. So, these instabilities could be minimized if we are having their in-depth knowledge. In 1962, Askaryan initially identified phenomenon of self-focusing [18]. The other nonlinear processes are directly affected due to self-focusing phenomena. Self-focusing process causes in change in dielectric and optical properties of plasma medium. Further, there is displacement of plasma electrons towards less intense portion as a result of ponderomotive mechanism in collisionless plasma. This in fact results in carrier redistribution in plasma. In laser-plasma interaction, generation of harmonics play a major role. The generation of harmonics is greatly influences propagation of lasers through plasma medium. The power of beam gets penetrated in the overdense portion as a result of production of harmonics. The harmonics production is valuable tool for retrieving information about pivotal parameters like expansion velocity, electron density, and opacity [19-20]. SHG helps in tracking transition of laser beam through plasma targets. The pulse duration of radiations of 2nd harmonics is very small. This really makes them suitable for plenty applications in UV spectroscopy [21-24]. The harmonics can be produced in laser produced plasmas through many techniques such as excitation of EPW, acceleration of photons, induced density gradients etc. [25-29]. The most frequently way of producing 2nd harmonics is with the help of excitation process of EPW. The production of density gradients in plasmas causes EPW excitation at pump wave frequency. The interaction of excited EPW with pump beam generates 2nd harmonics. Researchers have investigated SHG both theoretically and experimentally in the past [30-36]. It is quite clear from literature review that majority research on SHG has been explored in classical plasmas, which have less density and high temperature. Recently, a new plasma regime known as quantum plasmas has been explored. This regime has less temperature and high density. Researchers are highly motivated in exploring lasers interaction with quantum regime as a result of its applicability to plenty applications such as fusion science, nanotechnology, astrophysics etc. [37-42]. Further, nonlinear effects get amplified due to quantum effects. If the plasma temperature, Fermi temperature are denoted by T and T_F respectively. Then, quantum contribution can be expressed through parameter $\chi = \frac{T_F}{T}$. For $\chi \geq 1$, quantum effects become more pronounced. One can get overall details of quantum plasmas through FD-statistics. The De-Broglie wavelength λ_B differentiates quantum regime from classical regime. For the case of classical plasmas, λ_B has a very low value. Whereas, for quantum plasmas $\lambda_B \geq$ interatomic distance. Most of the research on SHG is either done through classical plasmas or through cylindrical Gaussian beams. In current study, we are exploring for the first time SHG of elliptical laser beam through TQP under

Cite as: K. Walia, K. Singh, A. Vijay, D. Tripathi, East Eur. J. Phys. 4, 542 (2025), https://doi.org/10.26565/2312-4334-2025-4-56

combined influence of RP force. The elliptical beam introduces anisotropy in self-focusing, an unequal waists along two transverse axes produce non-uniform intensity and asymmetric plasma density redistribution. This modifies local refractive index and phase matching for SHG. In Section 2, The well-established WKB and Paraxial theory are used for deriving 2nd order ODE for semi-major axis and semi-minor axis of laser beam having elliptical cross-section. In Section 3, we derived expression for the amplitude of EPW which act as 2nd harmonic source equation. The efficiency of second harmonics is derived in Section 4. In Section 5, detailed discussion of the results obtained is discussed and finally conclusion of results obtained is discussed in Section 6.

2. EVOLUTION OF SPOT SIZE OF LASER BEAM

Consider a laser beam having elliptical cross-section be transiting along z-axis. We have taken the transition of elliptical laser beam in TQP along z-axis. The present study incorporates both relativistic & ponderomotive nonlinear effects. Field amplitude for elliptical beams is taken as

$$E = E_0 exp\left(-\frac{x^2}{2a^2} - \frac{y^2}{2b^2}\right) \tag{1}$$

In Eq. (1), a & b denote initial beam radii of the semi-major axis and semi-minor axis respectively. E_0 is the maximum field amplitude. For, isotropic plasmas i.e, $J = 0, \rho = 0, \mu = 0$ the expressions for Faraday's law and Ampere's law becomes

$$\nabla \times B = \frac{1}{c}\frac{\partial D}{\partial t} \tag{2}$$

$$\nabla \times E = -\frac{1}{c}\frac{\partial B}{\partial t} \tag{3}$$

In Eqs. (2) & (3), E, B & $D = \varepsilon E$ correspond to electric vector, magnetic vector and electric displacement vector respectively. One can combine Eqs. (2) & (3) to obtain wave equation for electric vector as

$$\nabla^2 E - \nabla(\nabla \cdot E) + \frac{\omega^2}{c^2}\varepsilon E = 0 \tag{4}$$

In Eq. (4), we can ignore the term $\nabla(\nabla \cdot E)$ assuming that $\frac{1}{k^2}|\nabla^2 ln \in| \ll 1$ with k being propagation vector. Here, ω & ε correspond to angular frequency and dielectric function respectively. One can re-write Eq. (4) as

$$\nabla^2 E + \frac{\omega^2}{c^2}\varepsilon E = 0 \tag{5}$$

Under the joint contribution of quantum effects, Fermi pressure, and Bohm potential, the overall dielectric function for TQP takes the form [42-43]

$$\epsilon = 1 - \frac{\omega_p^2}{\gamma\omega^2}\left(1 - \frac{k^2 v_f^2}{\omega^2} - \frac{\delta q}{\gamma}\right)^{-1} \tag{6}$$

In Eq.(6), $v_f = \sqrt{\frac{2K_B T_f}{m}}$ denotes Fermi speed, γ is relativistic factor expressed as $\gamma = (1 + \alpha E E^*)^{1/2}$, and $\delta q = \frac{4\pi^4 h^2}{m^2\omega^2\lambda^4}$ respectively. If we substitute $T_f \rightarrow 0$ in Eq. (6), then we get ϵ for cold quantum plasma (CQP). Further, setting $T_f \rightarrow 0$, $\frac{h}{2\pi} \rightarrow 0$ in Eq. (6), we get ϵ for classical relativistic plasma (CRP). Further, $\omega_p = \sqrt{\frac{4\pi n e^2}{m}}$ denotes plasma frequency. The electron number density gets modified due to ponderomotive force. One can express this changed number density as [42-43]

$$n = n_0 exp\left(-\frac{mc^2}{T}(\gamma - 1)\right) \tag{7}$$

The general form for ε for TQP can be expressed as

$$\varepsilon = \varepsilon_0 + \varphi(E E_0^*) \tag{8}$$

In Eq. (8), the linear and nonlinear parts of ε can be expressed as $\varepsilon_0 = 1 - \frac{\omega_p^2}{\omega_0^2}$ & $\Phi(EE^*)$ respectively. Under combined action of RP force, the nonlinear part $\Phi(EE^*)$ of the dielectric function in TQP becomes

$$\Phi(EE^*) = \frac{\omega_{p0}^2}{\omega^2}\left[1 - \frac{1}{\gamma}\left(1 - \frac{k^2 v_f^2}{\omega^2} - \frac{\delta q}{\gamma}\right)^{-1} \exp\left(-\frac{mc^2}{T}(\gamma - 1)\right)\right] \tag{9}$$

Where $\omega_{p0} = \sqrt{\frac{4\pi n_0 e^2}{m}}$.

Following [44-45], the solution of Eq. (5) can be represented as

$$E = E_0 \exp\left[i\left(\omega t - k(S+z)\right)\right] \tag{10}$$

$$E_0^2 = \frac{E_{00}^2}{f_1 f_2} exp\left[-\frac{x^2}{a^2 f_1^2} - \frac{y^2}{b^2 f_2^2}\right] \tag{11}$$

$$S = \frac{x^2}{2}\beta_1(z) + \frac{y^2}{2}\beta_2(z) + \Phi_0(z) \tag{12}$$

$$k = \frac{\omega}{c}\sqrt{\varepsilon_0} \tag{13}$$

'S' represents eikonal for the beam with elliptical cross-section, $\beta_1(z) = \frac{1}{f_1}\frac{df_1}{dz}$ and $\beta_2(z) = \frac{1}{f_2}\frac{df_2}{dz}$ denote wavefront's curvature along X & Y axes respectively, $\Phi_0(z)$ is phase shift connected with beam, f_1 & f_2 denote beam widths of beam having elliptical cross-section and satisfy following 2nd order differential equations

$$\frac{d^2 f_1}{d\eta^2} = \frac{1}{f_1^3} - \left(\frac{\omega_p a}{c}\right)^2 \frac{\alpha E_{00}^2}{2 f_1^2 f_2} \frac{exp\left(-\frac{mc^2}{T_e}\left[\sqrt{1+\frac{\alpha E_{00}^2}{f_1 f_2}}-1\right]\right)}{\left(1+\frac{\alpha E_{00}^2}{f_1 f_2}\right)^{3/2}\left(1-\frac{k^2 v_f^2}{\omega^2}-\frac{\delta q}{\sqrt{1+\frac{\alpha E_{00}^2}{f_1 f_2}}}\right)^2}\left[\left(1-\frac{k^2 v_f^2}{\omega^2}\right)+\frac{mc^2}{T_e}\sqrt{1+\frac{\alpha E_{00}^2}{f_1 f_2}}\left(1-\frac{k^2 v_f^2}{\omega^2}-\frac{\delta q}{\sqrt{1+\frac{\alpha E_{00}^2}{f_1 f_2}}}\right)\right] \tag{14}$$

$$\frac{d^2 f_2}{d\eta^2} = \frac{a^4}{b^4 f_2^3} - \left(\frac{\omega_p a}{c}\right)^2 \frac{\alpha E_{00}^2}{2 f_2^2 f_1}\left(\frac{a}{b}\right)^2 \frac{exp\left(-\frac{mc^2}{T_e}\left[\sqrt{1+\frac{\alpha E_{00}^2}{f_1 f_2}}-1\right]\right)}{\left(1+\frac{\alpha E_{00}^2}{f_1 f_2}\right)^{3/2}\left(1-\frac{k^2 v_f^2}{\omega^2}-\frac{\delta q}{\sqrt{1+\frac{\alpha E_{00}^2}{f_1 f_2}}}\right)^2}\left[\left(1-\frac{k^2 v_f^2}{\omega^2}\right)+\frac{mc^2}{T_e}\sqrt{1+\frac{\alpha E_{00}^2}{f_1 f_2}}\left(1-\frac{k^2 v_f^2}{\omega^2}-\frac{\delta q}{\sqrt{1+\frac{\alpha E_{00}^2}{f_1 f_2}}}\right)\right] \tag{15}$$

In Eqs. (14) & (15), $\eta = z/ka^2$ is dimensionless propagation distance. Here, ka^2 denotes the Rayleigh length of beam. The boundary conditions selected for numerical calculation of these equations are $f_1 = f_2 = 1$ and $\frac{df_1}{d\eta} = \frac{df_2}{d\eta} = 0$ at $\boldsymbol{\eta} = 0$.

3. EXCITATION PROCESS OF EPW

We are incorporating motion of plasma electrons only for investigating excitation mechanism of EPW. Ions are excluded from excitation dynamics due to their heavy and immobile nature. The relativistic-ponderomotive force causes density fluctuations leading to excitation process of EPW. An analysis of the EPW excitation mechanism can be carried out through the following well-known standard equations;

(a) Continuity Equation

$$\frac{\partial N_e}{\partial t} + \nabla \cdot (N_e V) = 0 \tag{16}$$

(b) Poisson's Equation

$$\nabla \cdot E = 4\pi(ZN_{oi} - N_e)e \tag{17}$$

(c) Equation of State

$$\frac{P}{N_e^{\gamma}} = Constant \tag{18}$$

(d) Equation of Motion

$$m\left[\frac{\partial V}{\partial t} + (V\cdot\nabla)V\right] = -e\left[E + \frac{1}{c}V \times B\right] - 2\Gamma m V - \frac{\gamma}{N_e}\nabla P_e \tag{19}$$

Through the application of standard procedures, one arrives at the following equation for EPW:

$$-\omega_0^2 n_1 - v_{th}^2 \nabla^2 n_1 + 2\iota\Gamma\omega_0 n_1 + \omega_p^2\left[\frac{1}{\gamma}\left(1-\frac{k^2 v_f^2}{\omega^2}-\frac{h^2 k^4}{16\gamma\pi^2\omega^2 m^2}\right)^{-1}\exp\left(-\frac{mc^2}{T}(\gamma-1)\right)\right]^2 \quad n_1 \cong \frac{e}{m}\left(n_0 \vec{\nabla}.\vec{E}\right) \tag{20}$$

Incorporating Eq. (11) into Eq. (20) leads to the SHG source equation

$$n_1 = \frac{en_0}{m}\frac{E_{00}}{\sqrt{f_1 f_2}} exp\left(-\frac{x^2}{2a^2 f_1^2}\right) exp\left(-\frac{y^2}{2b^2 f_2^2}\right)\left(\frac{x}{a^2 f_1^2} + \frac{y}{b^2 f_2^2}\right)\frac{1}{\left\{\omega_0^2 - k^2 v_{th}^2 - \omega_p^2\left(\frac{1}{\gamma}\left(1-\frac{k^2 v_f^2}{\omega^2}-\frac{h^2 k^4}{16\gamma\pi^2\omega^2 m^2}\right)^{-1}\exp\left(-\frac{mc^2}{T}(\gamma-1)\right)\right)^2\right\}} \tag{21}$$

4. YIELD OF SECOND HARMONICS

Excited EPW interacts with main beam leading to SHG production. With Maxwell's equations as the foundation, one can obtain SHG field equation E_2 as

$$\nabla^2 E_2 + \frac{\omega_2^2}{c^2}\varepsilon_2(\omega_2)E_2 = \frac{\omega_p^2}{c^2}\frac{n_1}{n_0}E_0 \tag{22}$$

2nd harmonic radiations have frequency represented by $\omega_2 = 2\omega_0$ and dielectric function expressed as ε_2. The expression for E_2 can be written as

$$E_2 = \frac{\omega_p^2}{c^2}\frac{n_1}{n_0}\frac{E_{00}}{\sqrt{f_1 f_2}} exp\left(-\frac{x^2}{2a^2 f_1^2}\right) exp\left(-\frac{y^2}{2b^2 f_2^2}\right)\frac{1}{(k_2^2-4k^2)} \tag{23}$$

Now, SHG yield can be obtained as

$$Y_2 = \frac{\omega_p^4 e^2 E_{00}^2}{m_0^2 c^4 f_1 f_2} exp\left(-\frac{x^2}{a^2 f_1^2}\right) exp\left(-\frac{y^2}{b^2 f_2^2}\right)\left(\frac{x}{a^2 f_1^2}+\frac{y}{b^2 f_2^2}\right)^2 \frac{1}{(k_2^2-4k^2)^2}\frac{1}{\left\{\omega_0^2-k^2 v_{th}^2-\omega_p^2\left(\frac{1}{\gamma}\left(1-\frac{k^2 v_f^2}{\omega^2}-\frac{h^2 k^4}{16\gamma\pi^2\omega^2 m^2}\right)^{-1}\exp\left(-\frac{mc^2}{T}(\gamma-1)\right)\right)^2\right\}^2} \tag{24}$$

5. DISCUSSION

Since, it is not feasible to have analytical solution of Eqs. (14), (15) and (24). So, we have employed a numerical method. In fact, we have obtained accurate as well as stable solutions through fourth-order Runge–Kutta (RK4) method. In fact, RK4 is found to be best method for solving ordinary differential equations. We have employed established parameters for exploring the behavior of solutions as follows; $\alpha E_{00}^2 = 3.0, 4.0, 5.0$, $\frac{\omega_p^2}{\omega_0^2} = 0.4, 0.5, 0.6$, $T_f = 10^7 K, 10^8 K, 10^9 K$

The right side of Eqs. (14) and (15) contains two terms with distinct physical interpretations. In both equations, 1st terms belong to divergence effect thereby causing beam spreading, while 2nd terms belong to convergence effect thereby prompting beam focusing. During laser beam propagation inside plasma, these two terms govern overall evolution of beam width. When there is domination of 1st term, then beam spreading takes place leading to increase in its beam width. When there is domination of 2nd term, then beam focusing takes place leading to decrease in its beam width. When these opposing factors are exactly equal in magnitude, then we achieve self-trapping condition, where natural diffraction phenomenon is balanced by nonlinear focusing, maintaining a constant beam width.

Figures 1(a) & 1(b) illustrate variation of f_1 & f_2 as function of the normalized distance η for different laser intensity values $\alpha E_{00}^2 = 3.0, 4.0, 5.0$ respectively. Blue, green, and red color codes are used to denote $\alpha E_{00}^2 = 3.0, 4.0,$ and 5.0 respectively. The shifting of minimum values of f_1 & f_2 towards higher η is found with increasing αE_{00}^2 parameter. This indicates that beam focusing is delayed by higher laser intensity. In other words, beam's focusing efficiency is reduced with increasing αE_{00}^2 parameter. The observed trend is found due to diminished strength of the nonlinear focusing term in relation to the diffraction term as αE_{00}^2 parameter increases.

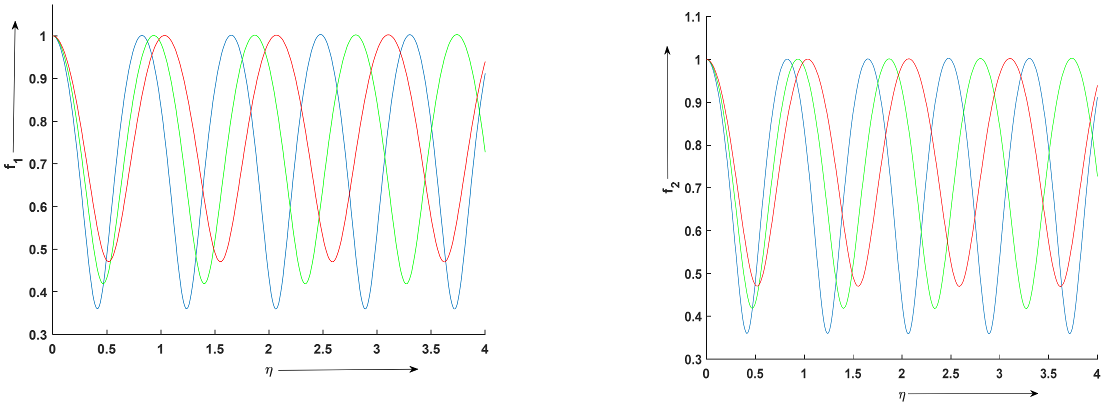

(a) (b)

Figure 1. Variation of f_1 & f_2 as function of the normalized distance η for different laser intensity values $\alpha E_{00}^2 = 3.0, 4.0, 5.0$ respectively. Blue, green, and red color codes are used to denote $\alpha E_{00}^2 = 3.0, 4.0,$ and 5.0 respectively

Figures 2(a) & 2(b) illustrate variation of f_1 & f_2 as function of the normalized distance η for different plasma density $\frac{\omega_p^2}{\omega_0^2} = 0.4, 0.5, 0.6$ respectively. Blue, green, and red color codes are used to denote $\frac{\omega_p^2}{\omega_0^2} = 0.4, 0.5,$ and 0.6 respectively. The shifting of minimum values of f_1 & f_2 towards smaller η is found with increasing $\frac{\omega_p^2}{\omega_0^2}$ parameter. This indicates that beam focusing is enhanced by higher plasma density. In other words, beam's focusing efficiency is enhanced with increasing $\frac{\omega_p^2}{\omega_0^2}$ parameter. The observed trend is found due to diminished strength of the diffraction term in relation to the nonlinear focusing term as $\frac{\omega_p^2}{\omega_0^2}$ parameter increases.

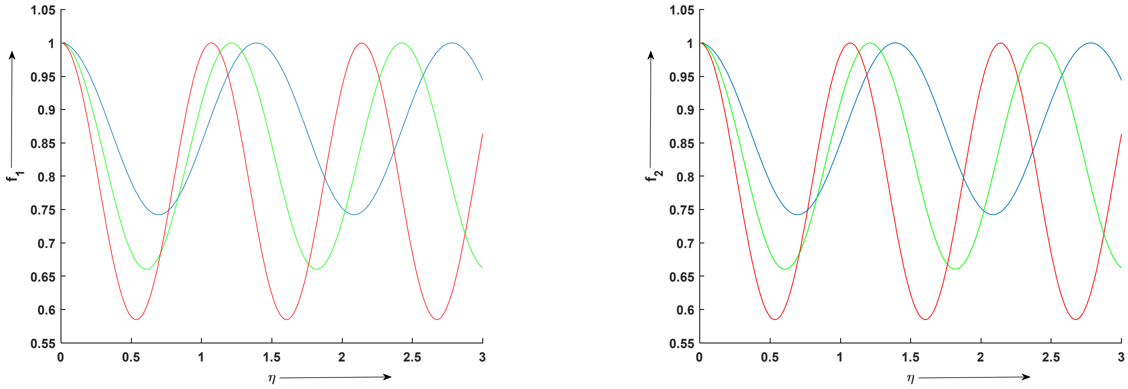

(a) (b)

Figure 2. Variation of f_1 & f_2 as function of the normalized distance η for different plasma density $\frac{\omega_p^2}{\omega_0^2} = 0.4, 0.5, 0.6$ respectively. Blue, green, and red color codes are used to denote $\frac{\omega_p^2}{\omega_0^2} = 0.4, 0.5,$ and 0.6 respectively

Figures 3(a) & 3(b) illustrate variation of f_1 & f_2 as function of the normalized distance η for different Fermi temperature $T_f\left(T_f = 10^7 K, 10^8 K, 10^9 K\right)$ respectively. Blue, green, and red color codes are used to denote $T_f = 10^7 K, 10^8 K, 10^9 K$ respectively. The shifting of minimum values of f_1 & f_2 towards smaller η is found with increasing T_f parameter. This indicates that beam focusing is enhanced by higher Fermi temperature. The higher Fermi temperature increases the Fermi pressure and electron degeneracy, leading to stronger plasma density redistribution. This enhances refractive index gradient and weakens diffraction spreading. As a result, nonlinear focusing effect dominates, causing the beam to self-focus more efficiently with increasing T_f.

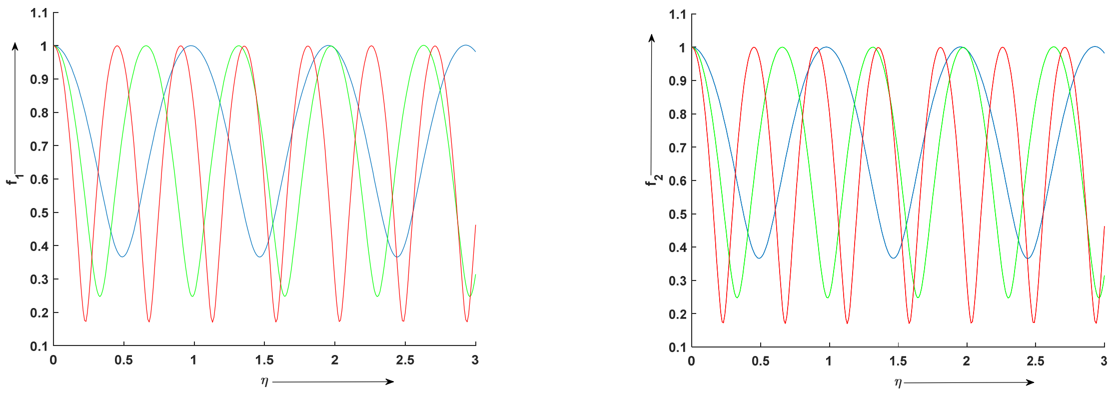

(a) (b)

Figure 3. Variation of f_1 & f_2 as function of the normalized distance η for different Fermi temperature $T_f\left(T_f = 10^7 K, 10^8 K, 10^9 K\right)$ respectively. Blue, green, and red color codes are used to denote $T_f = 10^7 K, 10^8 K, 10^9 K$ respectively

Figures 4(a) & 4(b) illustrate variation of f_1 & f_2 as function of the normalized distance η for different plasma regimes. Blue and red color codes are used for TQP and CRP cases. The more shifting of minimum values of f_1 & f_2 towards smaller η is found in TQP case as compared to CRP case. This indicates that beam focusing is enhanced by quantum effects. In other words, beam's focusing efficiency is enhanced with quantum contributions. Actually, quantum effects make the plasma respond more efficiently to intensity variations of laser beam, thereby enhancing nonlinear refractive index and promoting stronger self-focusing.

Figure 5 illustrates variation of SHG yield Y_2 as function of the normalized distance η for different laser intensity values $\alpha E_{00}^2 = 3.0, 5.0$ respectively. Blue and red color codes are used to denote $\alpha E_{00}^2 = 3.0$ and 5.0 respectively. It is found that the yield Y_2 gets reduced with decrease in αE_{00}^2. This reduction is attributed to the weaker self-focusing of the pump beam at higher αE_{00}^2 values. Since, magnitude of yield Y_2closely linked with effect of self-focusing, an increase in αE_{00}^2 leads to weaker self-focusing, thereby resulting in a reduced Y_2 value.

Figure 6 illustrates variation of SHG yield Y_2 as function of the normalized distance η for different plasma density $\frac{\omega_p^2}{\omega_0^2} = 0.4, 0.6$ respectively. Blue and red color codes are used to denote $\frac{\omega_p^2}{\omega_0^2} = 0.4$ and 0.6 respectively. It is found that the yield Y_2 gets enhanced with increase in $\frac{\omega_p^2}{\omega_0^2}$. This reduction is attributed to the stronger self-focusing of the pump beam at higher $\frac{\omega_p^2}{\omega_0^2}$ values. Since, magnitude of yield Y_2closely linked with effect of self-focusing, an increase in $\frac{\omega_p^2}{\omega_0^2}$ leads to stronger self-focusing, thereby resulting in higher Y_2 value.

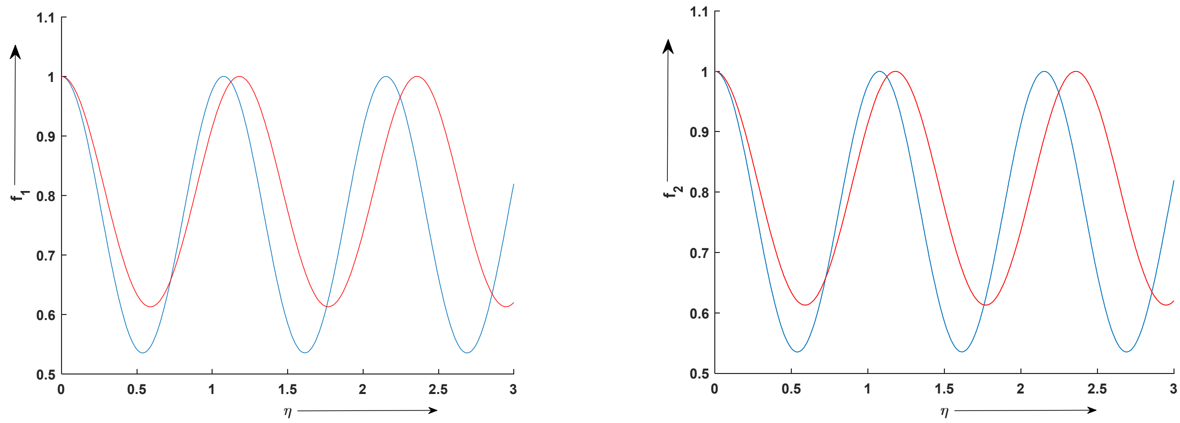

(a) (b)

Figure 4. Variation of f_1 & f_2 as function of the normalized distance η for different plasma regimes. Blue and red color codes are used for TQP and CRP cases

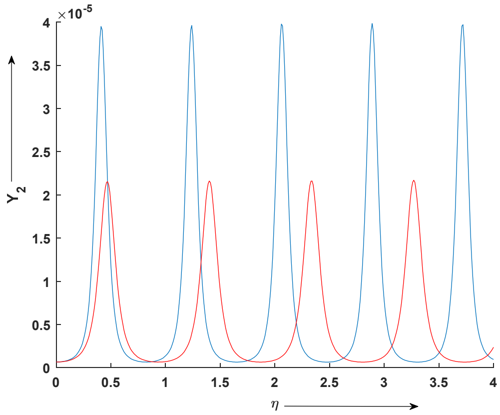

Figure 5. Variation of SHG yield Y_2 as function of the normalized distance η for different laser intensity values $\alpha E_{00}^2 = 3.0, 5.0$ respectively. Blue and red color codes are used to denote $\alpha E_{00}^2 = 3.0$ and 5.0 respectively

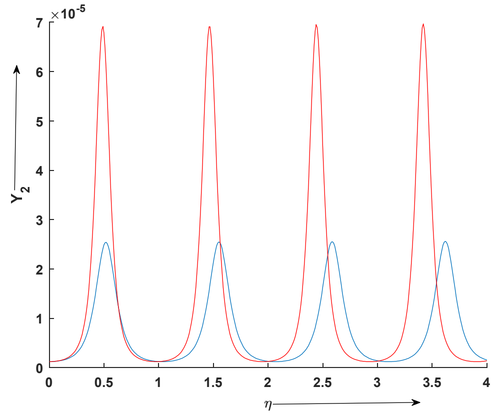

Figure 6. Variation of SHG yield Y_2 as function of the normalized distance η for different plasma density $\frac{\omega_p^2}{\omega_0^2} = 0.4, 0.6$ respectively. Blue and red color codes are used to denote $\frac{\omega_p^2}{\omega_0^2} = 0.4$ and 0.6 respectively

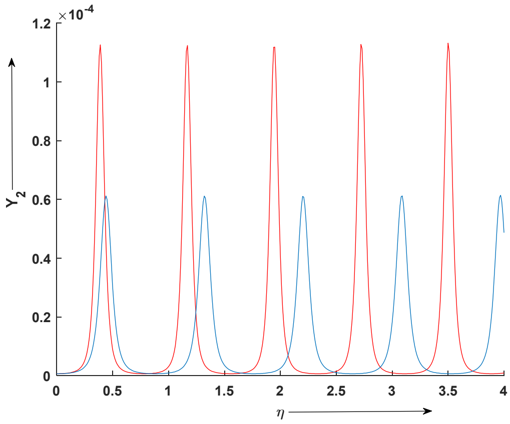

Figure 7. Variation of SHG yield Y_2 as function of the normalized distance η for different Fermi temperature $T_f\left(T_f = 10^7K, 10^9K\right)$ respectively. Blue and red color codes are used to denote $T_f = 10^7K$ and 10^9K respectively

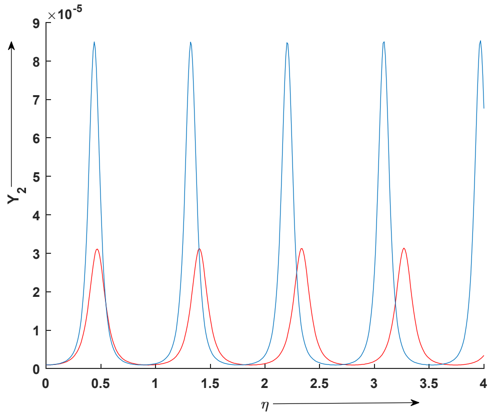

Figure 8. Variation of SHG yield Y_2 as function of the normalized distance η for different plasma regimes. Blue and red color codes are used to denote TQP and CRP respectively

Figure 7 illustrates variation of SHG yield Y_2 as function of the normalized distance η for different Fermi temperature $T_f\left(T_f = 10^7 K, 10^9 K\right)$ respectively. Blue and red color codes are used to denote $T_f = 10^7 K$ and $10^9 K$ respectively. It is found that the yield Y_2 gets enhanced with increase in T_f. This reduction is attributed to the stronger self-focusing of the pump beam at higher T_f values. Since, magnitude of yield Y_2closely linked with effect of self-focusing, an increase in T_f leads to stronger self-focusing, thereby resulting in higher Y_2 value.

Figure 8 illustrates variation of SHG yield Y_2 as function of the normalized distance η for different plasma regimes. Blue and red color codes are used to denote TQP and CRP respectively. In TQP, the value of Y_2 is significantly enhanced in comparison to CRP case. This enhancement is directly linked with process of self-focusing, as magnitude of Y_2 is strongly affected by self-focusing phenomenon. In Figures 7 & 8, beam focusing is found to be more dominant in TQP case followed by CRP case. Similar behavior is found for present study as well.

6. CONCLUSIONS

The current study explores SHG of elliptical laser beam in TQP. We have taken together relativistic and ponderomotive (RP) forces in current study. The results drawn from this study are mentioned below;

(1) There is increment in tendency of beam to focus with increase in $\frac{\omega_p^2}{\omega_0^2}$ and T_f parameters.
(2) The increase in αE_{00}^2 tends to reduction in beam focusing tendency.
(3) With inclusion of quantum effects, the beam exhibits better focusing characteristics.
(4) There is an enhancement in SHG yield Y_2 with enhancement in plasma density, Fermi temperature and with lowering in beam intensity values.
(5) The magnitude of Y_2 gets enhanced with inclusion of quantum effects.

These results are extremely useful for researchers exploring laser-plasma interaction physics.

ORCID
Keshav Walia, https://orcid.org/0000-0001-9547-3027; **Kulkaran Singh,** https://orcid.org/0000-0002-5982-8983
Deepak Tripathi, https://orcid.org/0000-0001-9945-4069; **Anuj Vijay,** https://orcid.org/0000-0001-6610-3844

REFERENCES

[1] S.C. Wilks, J.M. Dawson, W.B. Mori, T. Katsouleas, and M.E. Jones, "Photon accelerator," Phys. Rev. Lett. **62**, 2600 (1989). https://doi.org/10.1103/physrevlett.62.2600
[2] K.A. Brueckner, and S. Jorna, "Laser-driven fusion," Rev. Mod. Phys. **46**, 325(1974). https://doi.org/10.1103/RevModPhys.46.325
[3] J. Faure, Y. Glinec, A. Pukhov, S. Kiselev, S. Gordienko, E. Lefebvre, J.P. Rousseau, *et al.*, "A laser-plasma accelerator producing monoenergetic electron beams," Nature, **431**, 541(2004). https://doi.org/10.1038/nature02963
[4] P.E. Young, H.A. Baldis, R.P. Drake, E.M. Campbell, and K.G. Estabrook, "Direct Evidence of Ponderomotive Filamentation in a Laser-Produced Plasma," Phys. Rev. Lett. **61**, 2336 (1988). https://doi.org/10.1103/physrevlett.61.2336
[5] K. Walia, "Self-focusing of q-Gaussian beam in unmagnetized plasma and its impact on second harmonic generation," Optik, **277**, 170681 (2023). https://doi.org/10.1016/j.ijleo.2023.170681
[6] A. Singh, and K. Walia, "Relativistic self-focusing and self-channeling of Gaussian laser beam in plasma," Appl. Phys. B Lasers Opt. **101**, 617 (2010). https://doi.org/10.1007/s00340-010-4230-4
[7] P.B. Corkum, C. Rolland, and T. Rao, "Supercontinuum Generation in Gases," Phys. Rev. Lett. **57**, 2268 (1986). https://doi.org/10.1103/physrevlett.57.2268
[8] P. Sprangle, E. Esarey, and J. Krall, "Laser driven electron acceleration in vacuum, gases, and plasmas," Phys. Plasmas, **3**, 2183 (1996). https://doi.org/10.1063/1.871673
[9] W.F. Utlaut, and R. Cohen, "Modifying the ionosphere with intense radio waves," Science, **174**, 245(1971). https://doi.org/10.1126/science.174.4006.245
[10] K. Walia, "Nonlinear Interaction of High Power Elliptical Laser Beam with Cold Collisionless Plasma," J. Fusion Energ. **35**, 446 (2016). https://doi.org/10.1007/s10894-016-0059-0
[11] P. Kaw, G. Schmidt, and T. Wilcox, "Filamentation and trapping of electromagnetic radiation in plasmas," Phys. Fluids, **16**, 1522 (1973). https://doi.org/10.1063/1.1694552
[12] A. Bers, I.P. Shkarofsky, and M. Shoucri, "Relativistic Landau damping of electron plasma waves in stimulated Raman scattering," Physics of Plasmas. **16**, 022104 (2009). https://doi.org/10.1063/1.3073678
[13] D. Tripathi, T. Singh, A. Vijay, and K. Walia, "Second Harmonic Generation of q-Gaussian Laser Beam in Thermal Quantum Plasma," J. Contemp. Phys. **60**, 171(2025). https://doi.org/10.1134/s1068337225700574
[14] K. Walia, "Propagation characteristics of a high-power beam in weakly relativistic-ponderomotive thermal quantum plasma," Commun. Theor. Phys. **75**, 95501 (2023). https://doi.org/10.1088/1572-9494/accf82
[15] K. Walia, "Nonlinear interaction of high power beam in weakly relativistic and ponderomotive cold quantum plasma," Optik, **219**, 165040 (2020). https://doi.org/10.1016/j.ijleo.2020.165040
[16] C. Deutsch, A. Bret, M.C. Firpo, L. Gremillet, E. Lefebvre, and A. Lifschitz, "Onset of coherent electromagnetic structures in the relativistic electron beam deuterium-tritium fuel interaction of fast ignition concern," Laser Part. Beams, **26**, 157 (2008). https://doi.org/10.1017/s0263034608000189
[17] D. Tripathi, S. Kaur, A. Vijay, and K. Walia, "Nonlinear Dynamics of q-Gaussian Laser Beam in Collisional Plasma: Effect of Linear Absorption," J. Contemp. Phys. **60**, 16 (2025). https://doi.org/10.1134/s1068337225700409
[18] G.A. Askaryan, "Effects of the Gradient of a Strong Electromagnetic Beam on Electrons and Atoms," JETP, **15**, 1088 (1962).
[19] U. Teubner, and P. Gibbon, "High-order harmonics from laser-irradiated plasma surfaces," Rev. Mod. Phys. **8**, 445 (2009). https://doi.org/10.1103/revmodphys.81.445

[20] J.A. Stamper, R.H. Lehmberg, A. Schmitt, M.J. Herbst, F.C. Young, J.H. Gardner, and S.P. Obenschain, "Evidence in the second-harmonic emission for self-focusing of a laser pulse in a plasma," Phys. Fluids, **28**, 2563–2569 (1985). https://doi.org/10.1063/1.865264
[21] C. Winterfeldt, C. Spielmann, and G. Gerber, "Optimal control of high-harmonic generation," Rev. Mod. Phys. **80**, 117 (2008). https://doi.org/10.1103/revmodphys.80.117
[22] L. Nugent-Glandorf, M. Scheer, D.A. Samuels, A.M. Mulhisen, E.R. Grant, X. Yang, V.M. Bierbaum, and S.R. Leone, "Ultrafast Time-Resolved Soft X-Ray Photoelectron Spectroscopy of Dissociating Br," Phys. Rev. Lett. **87**, 193002 (2001). https://doi.org/10.1103/physrevlett.87.193002
[23] R.I. Tobey, M.E. Siemens, O. Cohen, M.M. Murnane, H.C. Kapteyn, and K.A. Nelson, "Ultrafast extreme ultraviolet holography: dynamic monitoring of surface deformation," Opt. Lett. **32**, 286-288 (2007). https://doi.org/10.1364/OL.32.000286
[24] M. Bauer, C. Lei, K. Read, R. Tobey, J. Gland, M.M. Murnane, and H.C. Kapteyn, "Direct observation of Surface Chemistry Using Ultrafast Soft-X-Ray Pulses," Phys. Rev. Lett. **87**, 025501 (2001). https://doi.org/10.1103/physrevlett.87.025501
[25] M.S. Sodha, J.K. Sharma, D.P. Tewari, R.P. Sharma, and S.C. Kaushik, "Plasma wave and second harmonic generation," Plasma Phys. **20**, 825 (1978). https://doi.org/10.1088/0032-1028/20/8/007
[26] J. Parashar, and H.D. Pandey, "Second-harmonic generation of laser radiation in a plasma with a density ripple," IEEE Trans. Plasma Sci. **20**, 996 (1992). https://doi.org/10.1109/27.199564
[27] F. Brunel, "Harmonic generation due to plasma effects in a gas undergoing multiphoton ionization in the high-intensity limit," J. Opt. Soc. Am. B, **7**, 521 (1990). https://doi.org/10.1364/josab.7.000521
[28] K. Singh, and K. Walia, "Second Harmonic Generation of High Power Cosh-Gaussian Beam in Thermal Quantum Plasma: Effect of Relativistic and Ponderomotive Nonlinearity," J. Contemp. Phys. **59**, 244 (2024). https://doi.org/10.1134/s1068337224700488
[29] K. Singh, and K. Walia, "Influence of Self-Focused Elliptical Laser Beam on Second Harmonic Generation in Cold Quantum Plasma," J. Contemp. Phys. **59**, 154 (2024). https://doi.org/10.1134/s1068337224700300
[30] K. Walia, N. Mehra, and S. Pandit, "Propagation Characteristics of q-Gaussian Laser Beam in Cold Collisionless Plasma," J. Contemp. Phys. **59**, 378 (2024). https://doi.org/10.1134/s1068337225700203
[31] K. Walia, "Effect of self-focusing of elliptical laser beam on second harmonic generation in collisionless plasma," Optik, **127**, 6618 (2016). https://doi.org/10.1016/j.ijleo.2016.04.043
[32] S. Kaur, A.K. Sharma, and H.A. Salih, "Resonant second harmonic generation of a Gaussian electromagnetic beam in a collisional Magnetoplasma," Phys. Plasmas, **16**, 042509 (2009). https://doi.org/10.1063/1.3135230
[33] N.H. Burnett, H.A. Baldis, M.C. Richardson, and G.D. Enright, "Harmonic generation in CO_2 laser target interaction," Appl. Phys. Lett. **31**, 172 (1977). https://doi.org/10.1063/1.89628
[34] R.L. Carman, D.W. Forslund, and J.M. Kindel, "Visible Harmonic Emission as a Way of Measuring Profile Steepening," Phys. Rev. Lett. **46**, 29 (1981). https://doi.org/10.1103/physrevlett.46.29
[35] T. Singh, and K. Walia, "Impact of High-Power Cosh-Gaussian Beam on Second Harmonic Generation in Collisionless Magnetoplasma," J. Contemp. Phys. **59**, 254 (2024). https://doi.org/10.1134/s106833722470049x
[36] N. Kant, and A.K. Sharma, "Effect of pulse slippage on resonant second harmonic generation of a short pulse laser in a plasma," J. Phys. D: Appl. Phys. **37**, 998 (2004).
[37] E. Ozbay, "Plasmonics: merging photonics and electronics at nanoscale dimensions," Science, **311**, 189 (2006). https://doi.org/10.1126/science.1114849
[38] L. Wei, and Y. Wang, "Quantum ion-acoustic waves in single-walled carbon nanotubes studied with a quantum hydrodynamic model," Phys. Rev. B, **75**, 193407 (2007). https://doi.org/10.1103/physrevb.75.193407
[39] G. Shpatakovskaya, "Semiclassical model of a one-dimensional quantum dot," J. Exp, Theor. Phys. **102**, 466 (2006). https://doi.org/10.1134/s1063776106030095
[40] Z. Chunyang, L. Zhanjun, Z. Shao-ping, and H. Xiantu, "Self-Focusing of High-Power Laser Beam through Plasma," J. Plasma Fusion Res. **6**, 333 (2004).
[41] A.V. Andreev, "Self-consistent equations for the interaction of an atom with an electromagnetic field of arbitrary intensity," J. Exp, Theor. Phys. Lett. **72**, 238 (2000). https://doi.org/10.1134/1.1324018
[42] D. Lai, "Matter in strong magnetic fields," Rev. Mod. Phys. **73**, 629 (2001). https://doi.org/10.1103/revmodphys.73.629
[43] Y. Jung, and I. Murakami, "Quantum effects on magnetization due to ponderomotive force in cold quantum plasmas," Phys. Lett. A, **373**, 969 (2009). https://doi.org/10.1016/j.physleta.2009.01.024
[44] M.S. Sodha, A.K. Ghatak, and V.K. Tripathi, *Progress in Optics*, (North Holland, Amsterdam, 1976).
[45] S.A. Akhmanov, A. Sukhorukov, and R. Khokhlov, "Self-focusing and diffraction of light in a nonlinear medium," Sov. Phys. Uspekhi, **10**, 609 (1968).

ГЕНЕРАЦІЯ ДРУГОЇ ГАРМОНІКИ ПОТУЖНОГО ЕЛІПТИЧНОГО ПРОМЕНЯ В ТЕПЛОВІЙ КВАНТОВІЙ ПЛАЗМІ

Кешав Валья[1], Кулкаран Сінгх[1], Анудж Віджай[2], Діпак Тріпаті[3]
[1]Кафедра фізики, Університет DAV, Джаландхар, Індія
[2]Кафедра фізики, Університет GLA, Матхура (У.П.), Індія-281406
[3]Кафедра фізики, USAR, Університет Гуру Гобінд Сінгх Індрапрастха, кампус Східного Делі, Делі, Індія-110032

У цьому дослідженні досліджується генерація другої гармоніки еліптичного променя в тепловій квантовій плазмі (TQP) шляхом об'єднання релятивістсько-пондеромоторних (RP) сил. Спостерігається зміна маси електронів через силу РП, що призводить до зміни профілю фонової густини в напрямку, поперечному до основного променя. Основний промінь самофокусується. Встановлені градієнти густини збуджують електронну плазмову хвилю (ЕПХ) на частоті хвилі накачування. Збуджена ЕПХ додатково взаємодіє з хвилею накачування, створюючи генерацію другої гармоніки (ГДГ). Для отримання звичайних диференціальних рівнянь 2-го порядку для великої та малої напівосей еліптичного променя з нормалізованою дальністю поширення та ефективністю других гармонік використовуються широко прийняті наближення ВКБ та параксіальна теорія. Крім того, також досліджується вплив зміни відповідних параметрів лазерної плазми на динаміку перетяжки променя та ефективність других гармонік.

Ключові слова*: еліптичний поперечний переріз; квантова плазма; сила рп; електронна плазмова хвиля; параксіальна теорія; наближення ВКБ*